$\phi$ = isothermal Joule–Thomson coefficient, $(\partial H/\partial P)_T$, J mol$^{-1}$ bar$^{-1}$

$\phi^0$ = zero-pressure isothermal Joule–Thomson coefficient, J mol$^{-1}$ bar$^{-1}$

### Literature Cited


(1) Alkasab, K. A., Shah, J. M., Laverman, R. J., Budenholzer, R. A., *Ind. Eng. Chem. Fundam.*, **10**, 237 (1971).
(2) Alkasab, K. A., Budenholzer, R. A., *Rev. Sci. Instrum.*, **44**, 1561 (1973).
(3) Benedict, M., Webb, G. B., Rubin, L. C., *J. Chem. Phys.*, **8**, 334 (1940); *ibid.*, **10**, 747 (1942).
(4) Bishnoi, P. R., Robinson, D. B., *Can. J. Chem. Eng.*, **50**, 101 (1972).
(5) Cullen, E. J., Kobe, K. A., *AIChE J.*, **1**, 452 (1955).
(6) Curl, R. F., Jr., Pitzer, K. S., *Ind. Eng. Chem.*, **50**, 265 (1958).
(7) Dymond, J. H., Smith, E. B., "The Virial Coefficients of Gases", Clarendon Press, Oxford, 1969.
(8) Harrison, R. H., Moore, R. T., Douslin, D. R., *J. Chem. Eng. Data*, **18**, 131 (1973).
(9) Hopke, S., Lin, C.-J., paper presented at 76th National AIChE Meeting, March 10–13, Tulsa, Okla. 1974.
(10) Klaus, R. L., Van Ness, H. C., *AIChE J.*, **13**, 1132 (1967).
(11) Lydersen, A. L., Greenkorn, R. A., Hougen, O. A., *Univ. Wis. Eng. Exp. Stn. Rep.*, **No. 4** (1955).
(12) Mather, A. E., Katz, D. L., Powers, J. E., *Trans. Faraday Soc.*, **64**, 2939 (1968).
(13) Mather, A. E., Powers, J. E., Katz, D. L., *AIChE J.*, **15**, 111 (1969).
(14) Newitt, D. M., Pai, M. U., Kuloor, N. R., Huggill, J. A., "Thermodynamic Functions of Gases", Vol. 1, F. Din, Ed., 1961, p 102.
(15) Ng, H.-J., M.S. Thesis, University of Alberta, 1971.
(16) Ng, H.-J., Ph.D. Thesis, University of Alberta, 1975.
(17) Peterson, J. M., Wilson, G. M., *Proc. Annu. Conv., Gas Process. Assoc., Tech. Papers*, **53**, 57 (1974).
(18) Pocock, G., Wormald, C. J., *J. Chem. Soc., Faraday Trans. 1*, **71**, 705 (1975).
(19) Soave, G., *Chem. Eng. Sci.*, **27**, 1197 (1972).
(20) Starling, K. E., Han, M. S., *Hydrocarbon Process.*, **51** (5), 129 (1972).
(21) Vukalovich, M. P., Altunin, V. V., Bulle, Kh., Rasskazov, D. S., Ertel, D., *Therm. Eng.*, (*Engl. Trans.*), **16** (11), 99 (1969).
(22) Vukalovich, M. P., Bulle, Kh., Rasskazov, D. S., Ertel, D., *Therm. Eng.* (*Engl. Trans.*), **17** (6), 93 (1970).
(23) Vukalovich, M. P., Bulle, Kh., Ertel, D., *Russ. J. Phys. Chem.*, **46**, 1475 (1972).
(24) Wilson, G. M., DeVaney, W. E., "Mark V Computer Program", available from the Gas Processors Association, Tulsa, Okla.
(25) Yen, L. C., Alexander, R. E., *AIChE J.*, **11**, 334 (1965).


Received for review June 10, 1975. Accepted February 17, 1976.

# Solubility of Inorganic Gases in High-Boiling Hydrocarbon Solvents

**Kevin K. Tremper and John M. Prausnitz***
*Chemical Engineering Department, University of California, Berkeley, California 94720*

**Low-pressure solubilities have been measured for 19 gas–solvent pairs. Gases and solvents used were: ammonia, nitrogen, carbon monoxide, hydrogen sulfide, hydrogen chloride, carbon dioxide, and sulfur dioxide; *n*-hexadecane, diphenylmethane, bicyclohexyl, and 1-methylnaphthalene. For all pairs, data were obtained in the temperature range 25–200 °C. The accuracy of these data is better than 1%.**

Design of chemical processing equipment, especially in the petroleum industry, often requires accurate knowledge of gas solubilities in various solvents over a wide temperature range. However, reliable gas-solubility data are not plentiful and most experimental data have been taken at room temperature. In this work the solubilities of seven gaseous solutes were measured in four high-boiling hydrocarbon solvents in the temperature range 25–200 °C. The experimental apparatus, designed and built by Cukor, is described in detail elsewhere (*4*).

The impetus for this work is twofold. Two previous workers using this solubility apparatus (Cukor (*4, 5, 6*) and Chappelow (*2, 3*)) studied exclusively hydrocarbon solutes. Thus one purpose for this work is to add to the previously reported data the solubilities of several nonhydrocarbon gases. These gases were selected first, because of their industrial importance and second, because of their physical properties. The gases span a range of dipole moment while the hydrocarbon solvents vary in molecular structure and degree of saturation (surface to volume ratio), as shown in Tables II and III. The second purpose of this work is to supply a firm experimental basis from which to develop a widely applicable solubility theory.

### Experimental Section

The experimental apparatus and procedure are essentially the same as those described by Cukor (*4, 5*) and Chappelow (*2, 3*). The following is a brief summary of the apparatus and procedure.

Figure 1 shows the experimental apparatus which consists of five sections: (1) a degassing flask, D; (2) an equilibrium cell, enclosed by the dotted box; (3) a reservoir for degassed solvent, E; (4) a precision gas burette, F; and (5) a section for pressure measurement, shown in detail in Figure 2.

The equilibrium cell consists of two volume-calibrated cells; one for solvent A and one for gas B. They are separated by a calibration mark, b. The original cell was modified to allow it to be removed and interchanged with other cells, as discussed in Appendix I.

The experiment begins by degassing the solvent, by alternate freezing and thawing under vacuum. Five repetitions are sufficient to remove the dissolved gases in all cases. The solvent is then transferred to the equilibrium cell and circulated under vacuum for final degassing. The solvent level in A is adjusted to the calibration mark b by draining the excess into the collecting flask E. This flask is then removed and weighed. Since the volume of the liquid section of the cell is known, the initial mass of solvent in the cell is determined from the density at the starting temperature.

The temperature of the bath is raised to the highest desired and the solvent vapor pressure is measured and compared to the literature value. This vapor pressure measurement is a final check on the proper degassing of the solvent. The expanded solvent is again lowered to the calibration mark b. The collecting flask E is again removed and weighed to determine the mass of solvent occupying the solvent cell volume. A known amount of gas is now added to the cell from the precision gas burette F. Equilibrium is attained quickly by circulating the solvent through the vapor space with pump C. Equilibrium is achieved when the pressure in the cell no longer changes at constant temperature, usually in less than 2 h. With the mass of each component known, only the temperature and pressure need be measured to specify the system completely. Once the pressure is measured, the bath is lowered to the next desired temperature. Since the solvent has contracted below the calibration mark b, makeup

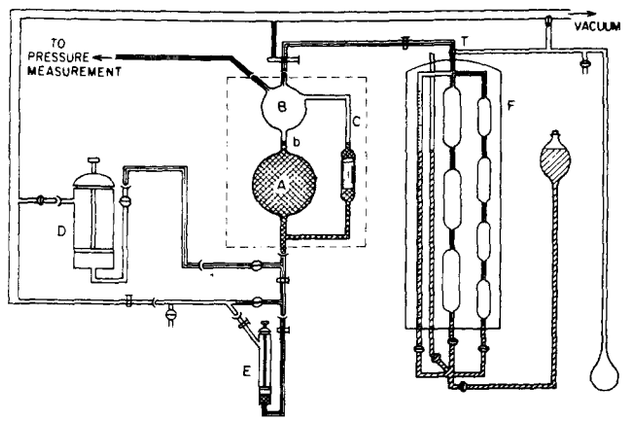


**Figure 1.** Gas-solubility apparatus.

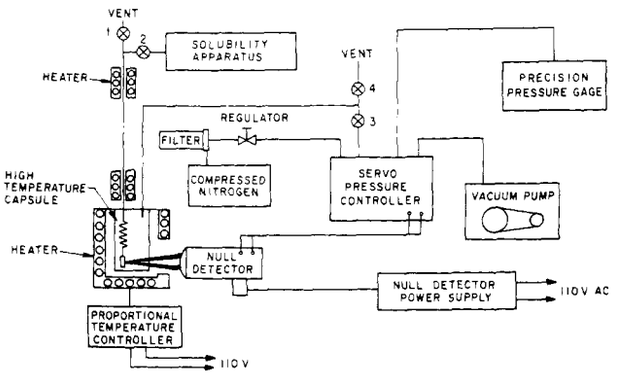


**Figure 2.** Measurement of pressure on condensable gases.

solvent is added from the collecting flask E. The flask is then removed and weighed. In this way the mass of solvent in the cell can always be determined by adding the difference in mass of the collecting flask E. The circulation pump is again started to attain equilibrium. After 2 h the pressure and temperature are measured, and the procedure is repeated at the next lower temperature.

The pressure gauge, shown in Figure 2, must always be maintained at a temperature equal to or greater that that of the equilibrium cell to prevent condensation in the gauge.

While all measurements were made at low pressures, experiments were made at several pressures to determine validity of Henry's law. Within experimental error, all solubility data used for final data reduction are within the Henry's-law region. Total pressures were always less than $10^3$ mmHg and usually much less.

**Table I. Henry's Constant and Entropy of Solution; Henry's Constant, atm (first line); Entropy of Solution (multiplied by minus one), cal/(mol K) (second line)**

| Gas | Liquid | Temperature, K 300 | 325 | 350 | 375 | 400 | 425 | 450 | 475 |
|---|---|---|---|---|---|---|---|---|---|
| Ammonia | *n*-Hexadecane | 45.8 | 59.0 | 73.4 | 87.6 | 100.0 | 112.0 | 122.0 | 129.0 |
| | | 6.38 | 6.13 | 5.49 | 4.65 | 3.86 | 3.22 | 2.66 | 2.25 |
| | Bicyclohexyl | 101.0 | 168.0 | 213.0 | 243.0 | 265.0 | 285.0 | 299.0 | 304.0 |
| | | 19.2 | 8.45 | 4.72 | 3.03 | 2.47 | 2.11 | 1.19 | 0.02 |
| | 1-Methylnaphthalene | 30.5 | 49.6 | 68.1 | 86.1 | 104.0 | 121.0 | 139.0 | 154.0 |
| | | 15.2 | 9.78 | 7.46 | 6.18 | 5.40 | 4.88 | 4.63 | 4.63 |
| Nitrogen | *n*-Hexadecane | 790.0 | 743.0 | 701.0 | 661.0 | 618.0 | 576.0 | 546.0 | 517.0 |
| | | −1.54 | −1.51 | −1.60 | −1.89 | −2.22 | −2.34 | −2.21 | −1.66 |
| | Diphenylmethane | 2937.0 | 2570.0 | 2304.0 | 2081.0 | 1890.0 | 1717.0 | 1553.0 | 1421.0 |
| | | −3.30 | −3.13 | −2.96 | −2.92 | −3.03 | −3.28 | −3.77 | −4.42 |
| | Bicyclohexyl | 1345.0 | 1274.0 | 1200.0 | 1123.0 | 1041.0 | 945.0 | 829.0 | 716.0 |
| | | −1.26 | −1.47 | −1.73 | −2.09 | −2.69 | −3.74 | −5.55 | −7.99 |
| | 1-Methylnaphthalene | 2970.0 | 2729.0 | 2481.0 | 2222.0 | 1949.0 | 1655.0 | 1338.0 | 1108.0 |
| | | −1.92 | −2.31 | −2.83 | −3.56 | −4.61 | −6.21 | −8.81 | −6.84 |
| Carbon monoxide | *n*-Hexadecane | 538.0 | 527.0 | 515.0 | 501.0 | 482.0 | 461.0 | 437.0 | 419.0 |
| | | −0.49 | −0.54 | −0.69 | −0.98 | −1.34 | −1.65 | −1.91 | −2.05 |
| | Bicyclohexyl | 975.0 | 981.0 | 980.0 | 967.0 | 937.0 | 885.0 | 806.0 | 723.0 |
| | | 0.18 | 0.08 | −0.17 | −0.63 | −1.36 | −2.47 | −4.19 | −5.67 |
| Hydrogen sulfide | *n*-Hexadecane | 25.2 | 32.6 | 40.9 | 49.7 | 58.9 | 68.0 | 76.6 | 82.7 |
| | | 6.61 | 6.21 | 5.85 | 5.44 | 4.97 | 4.42 | 3.80 | 3.24 |
| | Diphenylmethane | 32.9 | 43.9 | 56.2 | 70.1 | 86.1 | 104.0 | 123.0 | 132.0 |
| | | 7.61 | 6.80 | 6.45 | 6.32 | 6.32 | 6.38 | 4.69 | 1.18 |
| | Bicyclohexyl | 43.0 | 55.9 | 72.0 | 91.6 | 112.0 | 129.0 | 135.0 | 129.0 |
| | | 6.36 | 6.68 | 6.89 | 6.82 | 5.50 | 3.24 | −0.08 | −4.15 |
| | 1-Methylnaphthalene | 31.7 | 41.6 | 55.8 | 72.4 | 89.4 | 105.0 | 117.0 | 124.0 |
| | | 5.35 | 7.69 | 7.83 | 7.05 | 5.92 | 4.61 | 3.09 | 1.66 |
| Hydrogen chloride | *n*-Hexadecane | 45.0 | 54.3 | 65.8 | 78.3 | 90.7 | 102.0 | 111.0 | 116.0 |
| | | 4.06 | 5.06 | 5.14 | 4.81 | 4.22 | 3.47 | 2.52 | 1.61 |
| Carbon dioxide | *n*-Hexadecane | 74.3 | 93.2 | 112.0 | 129.0 | 144.0 | 157.0 | 168.0 | 176.0 |
| | | 6.00 | 5.24 | 4.49 | 3.74 | 3.11 | 2.62 | 2.21 | 1.94 |
| | Diphenylmethane | 123.0 | 161.0 | 196.0 | 228.0 | 259.0 | 287.0 | 309.0 | 306.0 |
| | | 7.42 | 5.80 | 4.81 | 4.13 | 3.62 | 3.22 | 1.31 | −2.48 |
| | Bicyclohexyl | 128.0 | 155.0 | 188.0 | 222.0 | 251.0 | 270.0 | 272.0 | 258.0 |
| | | 4.11 | 5.12 | 5.05 | 4.32 | 3.14 | 1.51 | −1.03 | −4.33 |
| | 1-Methylnaphthalene | 127.0 | 165.0 | 206.0 | 247.0 | 283.0 | 311.0 | 326.0 | 312.0 |
| | | 6.40 | 6.27 | 5.64 | 4.76 | 3.70 | 2.45 | 0.26 | −5.18 |
| Sulfur dioxide | *n*-Hexadecane | 15.1 | 22.3 | 30.8 | 40.2 | 50.1 | 60.1 | 69.8 | 77.1 |
| | | 10.1 | 9.17 | 8.15 | 7.21 | 63.6 | 5.58 | 4.82 | 4.22 |

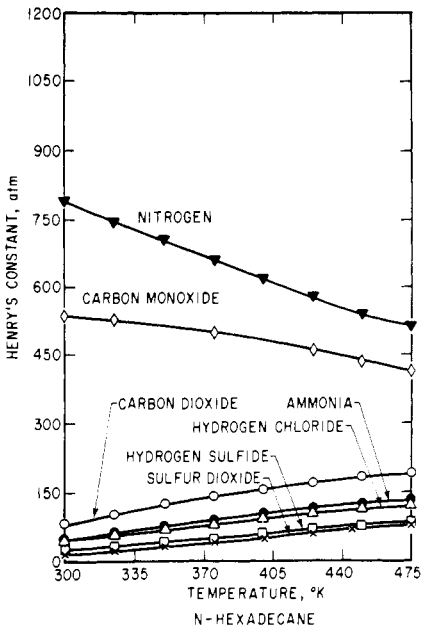


**Figure 3.** Henry's constants in *n*-hexadecane.

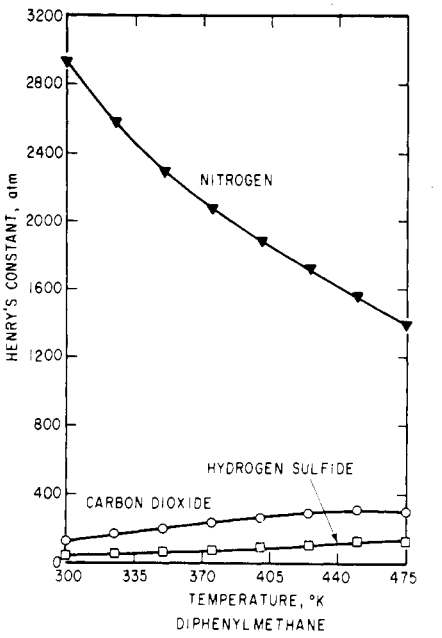


**Figure 5.** Henry's constants in diphenylmethane.

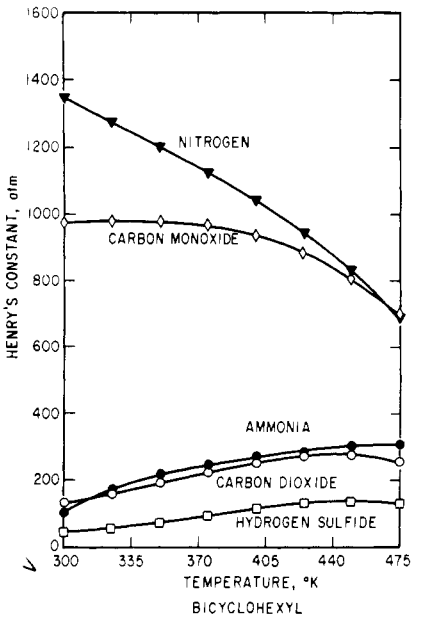


**Figure 4.** Henry's constants in bicyclohexyl.

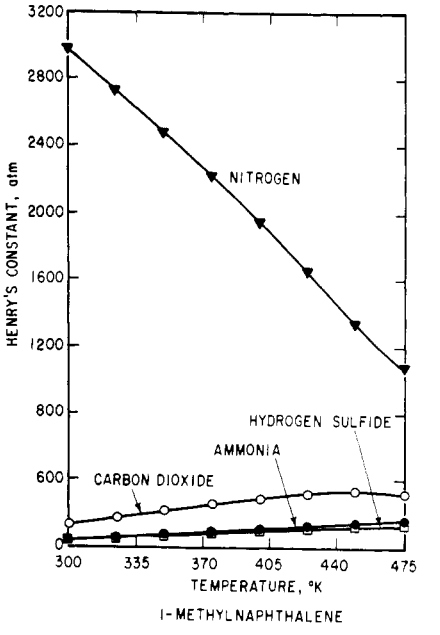


**Figure 6.** Henry's constants in 1-methylnaphthalene.

### Data Reduction

The solubility is calculated by determining the amount of solute remaining in the vapor phase. Since the number of moles added to the system is known, the amount dissolved in the solvent can be determined by difference. Let subscript 1 stand for the solute and subscript 2 for the solvent. The solubility is the liquid mole fraction of the solute, $x_1$. It is given by:

$$x_1 = \frac{\Delta n_1}{\Delta n_1 + \Delta n_2} \tag{1}$$

where $\Delta n_i$ is the moles of $i$ remaining in the liquid phase.

Henry's constant for solute 1 dissolved in solvent 2 is defined by:

$$H_{1,2} = \lim_{x_1 \to 0} \frac{f_1}{x_1} \tag{2}$$

where $f$ is fugacity.

Experimental measurements are the total pressure, calibrated volumes, temperature, and the number of moles of each component. To solve for Henry's constant, the equations of equilibrium are used for each component coupled with an equation of state for the vapor phase. The equations of equilibrium are:

$$\phi_1 y_1 P = H_{1,2} x_1 \tag{3}$$

$$\phi_2 y_2 P = x_2 P_2^s \tag{4}$$

where $\phi$ is the vapor-phase fugacity coefficient, $P$ is the total pressure, and $P_2^s$ is the solvent vapor pressure. The virial equation of state, truncated after the second term, is used to calculate the total number of moles in the vapor phase and the vapor-phase fugacity coefficients. The virial coefficients are calculated using the correlation of Pitzer and Curl (*7*) with mixing rules recommended by Prausnitz and Chueh (*9*).

Equations 3 and 4 are solved by trial-and-error as described by Chappelow (*2*).

**Table II. Solvent Properties**

| Solvent | Solubility parameter[a] (cal/cm$^3$)$^{1/2}$ at 25 °C | van der Waals[b] Volume (cm$^3$/mol) | van der Waals[b] Surface area $10^9$ (cm$^2$/mol) | Surface/volume ratio, $10^9$ (cm$^{-1}$) |
|---|---|---|---|---|
| *n*-Hexadecane | 8.00 | 170.56 | 23.14 | 0.1357 |
| Bicyclohexyl | 8.16 | 113.60 | 15.50 | 0.1364 |
| 1-Methylnaphthalene | 8.66 | 85.12 | 12.42 | 0.1456 |
| Diphenylmethane | 9.08 | 101.91 | 15.30 | 0.1501 |

[a] From Prausnitz (*8*); Cukor (*5*). [b] from Bondi (*1*).

**Table III. Normal Boiling Points and Dipole Moments of Solutes**

| Solute | Normal boiling point, K | Dipole moment, D |
|---|---|---|
| Nitrogen | 77.3 | 0 |
| Carbon monoxide | 81.7 | 0.10 |
| Hydrogen chloride | 188.2 | 1.08 |
| Carbon dioxide | 194.7 | 0 |
| Hydrogen sulfide | 211.4 | 0.92 |
| Ammonia | 239.8 | 1.47 |
| Sulfur dioxide | 263.2 | 1.61 |

Henry's constants and partial molar entropies of solution are given in Table I for 19 binary gas–liquid systems.

The partial molar entropy of solution is defined by:

$$\Delta\bar{s}_1 \equiv \bar{s}_1^{L}(T,x_1 = 1/H_{1,2}) - s^{G}_{\text{pure }1}(T,f_1 = 1 \text{ atm}) = -R\left(\frac{\text{d ln } H_{1,2}}{\text{d ln } T}\right) \quad (5)$$

where $\bar{s}_1^{L}$ is the partial molar entropy of solute 1 in the liquid phase, $H_{1,2}$ is Henry's constant in atmospheres, $T$ is absolute temperature, $x$ is mole fraction in the liquid phase, and $R$ is the gas constant. Superscripts L and G stand for liquid and ideal gas, respectively. The partial molar enthalpy of solution is defined in an analogous manner:

$$\Delta\bar{h}_1^{L} \equiv \bar{h}_1^{L}(T,x_1 = 1/H_{1,2}) - h_1^{G}(T,f_1 = 1 \text{ atm}) = R\left(\frac{\text{d ln } H_{1,2}}{\text{d}1/T}\right) \quad (6)$$

The partial molar enthalpy and partial molar entropy are simply related by

$$\Delta\bar{h}_1 = T\Delta\bar{s}_1 \quad (7)$$

Henry's constants are shown as a function of temperature in Figures 3, 4, 5 and 6.

## Discussion

For most gases at ordinary temperatures, the solubility decreases with rising temperature. This is expected because, as temperature rises, the kinetic energy of the gas becomes larger than that at its own normal boiling point and thus there is a decreasing tendency to condense into a liquid phase. However, as shown by data presented here and elsewhere (*3, 6, 8*) the solubilities of some gases increase with temperature while others first decrease and then increase. It appears likely that the solubilities of all gases first decrease, go through a minimum, and then increase if taken over a wide enough temperature range. The increase of solubility with temperature is probably

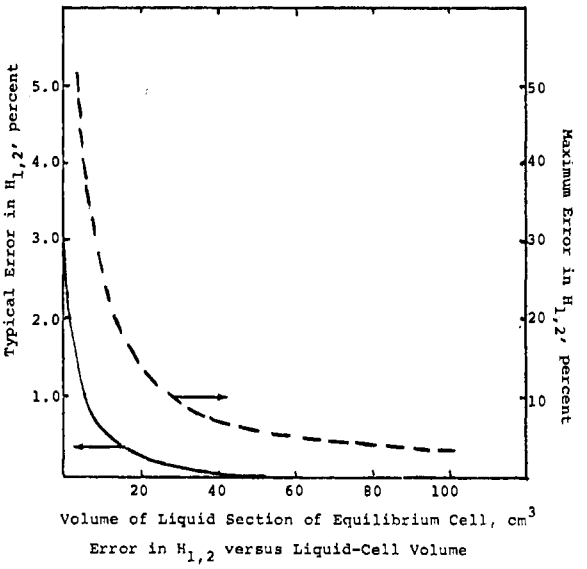


**Figure A1.**

related to the decrease in solvent density as temperature rises. Calculations by Preston (*10*) suggest that in simple systems, gas solubility decreases monotonically with temperature when the density of the solvent is held constant.

Some insight on the effect of temperature on solubility may be obtained by considering the partial molar entropy of solution in the Henry's-law limit. Rewriting eq 5 in terms of solubility, we obtain

$$\frac{\text{d ln } x_1}{\text{d ln } T} = \frac{\Delta\bar{s}_1}{R} \quad (8)$$

where $x_1$ is the mole-fraction solubility when the fugacity of the gaseous solute is 1 atm. The solution of a solute gas into a solvent liquid can be divided into a two-step process: isothermal compression of the gas to a "liquid-like" volume that it occupies when dissolved in the solute followed by isothermal mixing of the compressed solute with the solvent. The entropy change for this first step is usually negative and dominates at low temperatures while the entropy change for the second step is always positive and increases with decreasing solubility. Thus a point can be reached where the second term dominates and the solubility increases with rising temperature.

In nonpolar systems, solubilities follow unambiguous trends with the physical properties of the solute and solvent; solubility increases with solute normal boiling point (Table III) and decreases with solvent solubility parameter (Table II). However, the solubilities of polar gases also depend on the solute's dipole moment and on Lewis acid–base interactions.

Solute dipole moments (Table III) and solvent van der Waals volumes, surface areas, and surface-to-volume ratios (Table II) may facilitate interpretation of the data. Although hydrogen chloride is more soluble in *n*-hexadecane than carbon dioxide, hydrogen chloride has the lower boiling point. The large dipole moment of hydrogen chloride induces attractive interactions with the solvent thus increasing its solubility. The acidic (electron accepting) nature of hydrogen chloride causes additional attraction to basic (electron donating) solvents like diphenylmethane and $\alpha$-methylnaphthalene.

Ammonia and hydrogen sulfide are both more soluble in the aromatic solvents than in bicyclohexyl. Both gases have large interaction-inducing dipoles. The aromatic solvents have larger polarizabilities and larger surface-to-volume ratios allowing a greater interacting surface per electronegative carbon. The lack of hydrogens in the aromatics allows the inducing dipole solute to "get closer" to the carbon atoms. In unsaturated solvents the

carbons are surrounded by $\pi$-bonding rather than s-bonding electrons which characterize saturated hydrocarbons.

### Conclusion

The data presented here may be useful for engineering design where higher temperatures are increasingly encountered. Further, these data contribute toward the experimental information required to construct a successful theory of gas solubility.

### Appendix I. Minimum Cell Volume Error Analysis

Since some high-boiling solvents are costly, it is desirable to use a small solubility cell. Therefore, it is important to determine how small the solubility cell can be made without a large increase in experimental error. Further, some gases of scientific and industrial interest, e.g., hydrogen sulfide, are extremely toxic making it advisable to use as small an amount as possible.

The error in Henry's constants was calculated as a function of liquid cell volume for a typical case and for the worst case with respect to pairs of gases and high-boiling solvents. The worst case is for a very slightly soluble gas, e.g., hydrogen, in a solvent with high vapor pressure, e.g., octamethylcyclotetrasiloxane. The typical case is for the squalane–ethane system. Results are presented in Figure A1. From these results it was decided that, for expensive solvents and/or toxic solutes, we may use a new, interchangeable solubility cell with a liquid volume of between 30 and 40 $cm^3$. The cell used in previous work has a volume of 300 $cm^3$.

### Literature Cited


(1) Bondi, A., "Physical Properties of Molecular Crystals, Liquids, and Glasses", Wiley, New York, N.Y., 1968.
(2) Chappelow, C. C., Ph.D. Dissertation, University of California, Berkeley, 1974.
(3) Chappelow, C. C., Prausnitz, J. M., *AIChE J.*, **20,** 1097 (1974).
(4) Cukor, P. M., Prausnitz, J. M., *Ind. Eng. Chem. Fundam.*, **10,** 638 (1971).
(5) Cukor, P. M., Ph.D. Dissertation, University of California, Berkeley, 1971.
(6) Cukor, P. M., Prausnitz, J. M., *J. Phys. Chem.*, **76,** 598 (1972).
(7) Pitzer, K. S., Curl, R. F., *J. Am. Chem. Soc.*, **79,** 2394 (1957).
(8) Prausnitz, J. M., "Molecular Thermodynamics of Fluid Phase Equilibrium", Prentice-Hall, Englewood Cliffs, N.J., 1968.
(9) Prausnitz, J. M., Chueh, P. L., "Computer Calculations for High-Pressure Vapor-Liquid Equilibria", Prentice-Hall, Englewood Cliffs, N.J., 1968.
(10) Preston, G. T., Funk, E. W., Prausnitz, J. M., *Phys. Chem. Liq.* **2,** 193 (1971).



Received for review June 24, 1975. Accepted December 17, 1975. For financial support the authors are grateful to the American Petroleum Institute, the National Science Foundation, and the American Gas Association.


# Vapor–Liquid Equilibria in the Freon 12–Freon 13 System


**Jørgen Mollerup* and Aage Fredenslund***

*Instituttet for Kemiteknik, Danmarks tekniske Højskole, DK-2800 Lyngby, Denmark*



**Isothermal vapor–liquid equilibrium data were determined for the Freon 12–Freon 13 system at 255 and 290 K using a high-pressure vapor recirculation apparatus. The experimental vapor compositions are compared with those calculated from the *P–x* data on the basis of the Gibbs–Duhem equation. The two sets of vapor phase compositions are on the average found to be consistent within 0.01 mol fraction.**


Analysis of thermodynamic irreversibility in refrigeration cycles shows that for optimal efficiency (and thus minimal use of energy), the temperature difference between the refrigerant and the process stream must be small. Cooling cycles with mixed refrigerants can be designed to meet this requirement (*5*), provided the physical and thermodynamic properties of the mixtures can be predicted accurately. Thus experimental information on mixtures of refrigerants is of increasing practical importance, and this work gives isothermal vapor–liquid equilibrium data for the Freon 12($CCl_2F_2$)–Freon 13 ($CClF_3$) system at 255 K and 290 K. Vapor–liquid equilibrium data for this system have not been reported in the literature previously. Vapor-phase mole fractions ($y$) were calculated directly from the $P$–$x$ data without making use of the experimental $y$'s. The calculated and experimental $y$'s compare satisfactorily, and thus the data are thermodynamically consistent.

### Experimental Section

The Freons were obtained from Danfoss a/s and had a guaranteed purity of better than 99.8%. The impurities consisted mainly of partly halogenated methane. No further purification was performed. Published and experimental values of pure component physical properties are shown in Table I.

The experiments were carried out using a high-pressure vapor recirculation apparatus described in detail elsewhere (*3*). The cell contains a stationary liquid phase, and the vapor is circulated through the liquid using a diaphragm compressor. The cell volume is 50 $cm^3$ and the total vapor volume is roughly equal to that; about 3 $\mu$l of liquid is withdrawn per liquid sample, and roughly $2 \times 10^{-4}$ mol is used for each vapor sample. The temperature is measured and maintained to

**Table I. Pure-Component Parameters**

| Property | Freon 12 | Freon 13 |
|---|---|---|
| Vapor pressure at 255 K, atm | | |
| Measured | 1.602 | 11.902 |
| Lit. (*2*) | 1.601 | 11.920 |
| Vapor pressure at 290 K, atm | | |
| Measured | 5.096 | 29.288 |
| Lit. (*2*) | 5.127 | 29.593 |
| Critical temperature, K | 301.93 | 385.15 |
| Critical volume, $cm^3$/g mol | 179.8 | 216.7 |
| Critical pressure, atm | 38.144 | 41.032 |
| Acentric factor | 0.1695 | 0.1803 |
| Redlich–Kwong parameters[a] | | |
| $\Omega_A$ | 0.4216 | 0.4215 |
| $\Omega_B$ | 0.9361 | 0.08480 |
| Deviation from geometric mean: $1 - k_{12} = T_{12}^C(T_1^C \cdot T_2^C)^{-0.5}$ | $k_{12} = 0.03$ | |

[a] Redlich–Kwong equation of state: $P = [RT/(V - b)] - [(a/V)/\sqrt{T}(V + b)]$; $a = \Omega_A R^2 T_C^{2.5}/P_C$; $b = \Omega_B RT_C/P_C$.